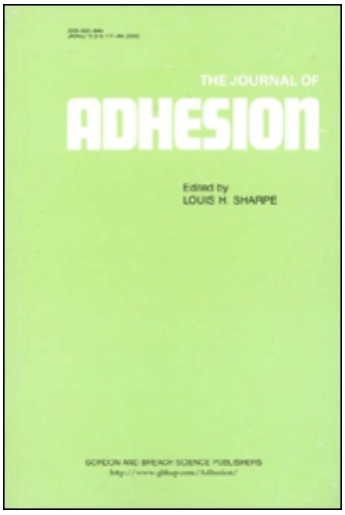

The Journal of Adhesion

Publication details, including instructions for authors and subscription information:
http://www.informaworld.com/smpp/title~content=t713453635

Surface-Force-Induced Nonelastic Deformations Between Micrometer Size Glass Particles and Silicon Substrates

R. C. Bowen[a]; L. P. Demejo[b]; D. S. Rimai[b]
[a] Analytical Technology Division, Eastman Kodak Company, Rochester, NY, U.S.A. [b] Image Research and Advanced Development, Eastman Kodak Company, Rochester, NY, U.S.A.

To cite this Article Bowen, R. C. , Demejo, L. P. and Rimai, D. S.(1995) 'Surface-Force-Induced Nonelastic Deformations Between Micrometer Size Glass Particles and Silicon Substrates', The Journal of Adhesion, 51: 1, 201 — 210
To link to this Article: DOI: 10.1080/00218469508009999
URL: http://dx.doi.org/10.1080/00218469508009999

J. Adhesion, 1995, Vol. 51, pp. 201–210
Reprints available directly from the publisher
Photocopying permitted by license only

Surface-Force-Induced Nonelastic Deformations Between Micrometer Size Glass Particles and Silicon Substrates*

R. C. BOWEN **

Analytical Technology Division, Eastman Kodak Company, Rochester, NY 14650-2151, U.S.A.

L. P. DEMEJO and D. S. RIMAI

Image Research and Advanced Development, Eastman Kodak Company, Rochester, NY 14650-2129, U.S.A.

(Received March 7, 1995; in final form April 24, 1995)

Glass beads having radii between 3 μm to 25 μm were gently deposited onto a polished silicon wafer, and the surface-force-induced particle-substrate contact radii were determined using scanning electron microscopy. The contact radii were found to vary as the particle radii to the 0.42 power (± 0.14), which is consistent with the plastic deformation model of Maugis and Pollock,[10] but inconsistent with the predictions of the elastic-response based adhesion models proposed by Johnson, Kendall, and Roberts[5] or Derjaguin, Muller, and Toporov.[6] Estimates of the stresses due to the surface forces suggest that they exceed the tensile strength of glass and that the observed deformations can arise from these tensile stresses.

KEY WORDS particle; glass; adhesion; deformation; JKR; contact area; SEM.

INTRODUCTION

The study of particle adhesion is a subject of interest to both the scientific and manufacturing communities. The cleaning of silicon wafers for the microelectronics industry, the adhesion of paint, and the deposition/removal of toner in xerography are but a few of the technological or practical examples of particle adhesion. Bradley[1,2] and Derjaguin[3] independently proposed that surface forces between particles and substrates can be significant enough to cause the particle or substrate to deform.

Derjaguin[3] assumed that these deformations can be described using a Hertzian indentor model,[4] with the applied load arising from van der Waals interactions. Johnson, Kendall, and Roberts (JKR)[5] recognized that, in addition to compressive forces, tensile forces also contribute to the size of the deformation. Accordingly, the contact radius, a, is related to the particle radius, R, the work of adhesion, w_a and the

* Presented in part at the Seventeenth Annual Meeting of The Adhesion Society, Inc., in Orlando, Florida, U.S.A., February 21–23, 1994.

** Corresponding author.

Young's moduli and Poisson ratios of the two materials, E_i and ν_i, by

$$a^3 = \frac{R}{K}\{P + 3w_a\pi R + [6w_a\pi RP + (3w_a\pi R)^2]^{1/2}\} \tag{1}$$

where P is the applied load and

$$K = \frac{4}{[3\pi(k_1 + k_2)]} \tag{2}$$

where

$$k_i = \frac{1 - \nu_i^2}{\pi E_i} \tag{3}$$

In the absence of an externally applied load, Equation (1) reduces to

$$a^3 = \frac{6w_a\pi R^2}{K} \tag{4}$$

Their work with soft gelatin and rubber spheres showed that, even with no externally applied load, the observed deformations were larger than could be accounted for by Derjaguin's model. Derjaguin, Muller, and Toporov (DMT)[6] incorporated tensile effects into Derjaguin's original work. However, as discussed by Tabor,[7] there are discrepancies between the JKR and DMT models. For example, the contact radius predicted by the DMT model is approximately half of that predicted by the JKR model. These differences were resolved by Muller, Yushchenko, and Derjaguin (MYD).[8] The DMT model was found to be more applicable to rigid, low surface energy materials, while the JKR model was more applicable to compliant, high surface energy materials. Both of these models assume that the deformations are elastic and predict that the contact radius varied as the particle radius to the 2/3 power.

Krupp[9] was the first to propose that the surface forces could be sufficiently large to cause plastic deformation of one or both of the contacting materials. Maugis and Pollock (MP)[10] generalized the JKR theory to include plastic deformations. According to the MP model, the contact radius, a, is related to the yield strength of the material, Y, and the radius of the particle, R, by

$$P + 2\pi w_a R = 3\pi a^2 Y \tag{5}$$

In the absence of any applied load, P, Equation (5) reduces to

$$a = \left(\frac{2w_a}{3Y}\right)^{1/2} R^{1/2} \tag{6}$$

The MP model assumes the deformations are nonelastic and predicts that the contact radius varies as the particle radius to the 1/2 power.

Therefore, by determining the power law dependence of the contact radius on the particle radius, it is possible to determine the nature of the deformation. Moreover, if the mechanical properties of the materials are known, the appropriate theory can be used to calculate properties such as the thermodynamic work of adhesion.

Scanning electron microscopy has recently been used in a number of studies to determine the surface-force-induced contact radii for a variety of particle-substrate

systems.[11-14] These studies typically involved gently depositing the spherical particles onto a substrate of choice, applying a 10 nm Au/Pd coating to minimize beam-induced space charge effects when viewed in the SEM, and examining the particle-substrate interface at high sample tilt. The "high tilt" technique has proven very useful, but it has limitations, particularly when the deformations are small compared with the particle radius. In this case, when the contact areas are small, it is frequently difficult to measure accurately the contact radii due to shadowing and other effects.

A new technique has been described[15] which addresses these concerns. This technique, referred to as the Contact Area Measurement (CAM) technique, involves evaporating a thin, uniform coating of aluminum onto a sample comprised of particles that were gently deposited onto a substrate. The sample is examined before and after particle removal to determine both the particle and contact radii. Where the particle contacted the substrate, no metallization occurred, and after particle removal, this provides a contrast mechanism that the SEM can image. The CAM technique allowed the measurement of the contact radius of micrometer size glass beads contacting a silicon substrate. The results of this study will now be discussed.

EXPERIMENTAL

Glass beads,[16] nominally ranging from 3 μm to 25 μm in radius, were gently deposited onto a polished silicon substrate by "sprinkling" the beads onto the substrate from a height of 1 cm. As previously discussed,[11] these conditions assured that minimal kinetic energy would be imparted to the beads, thereby reducing the probability of causing the contact areas to be larger than otherwise anticipated with no applied load.[17,18] Prior to coating or examination, the sample was allowed to equlibrate at ambient conditions for 7 days. One set of samples was coated with approximately 50 nm of aluminum in an Edwards high vacuum evaporator and examined using the CAM technique.[15] During coating, the sample was rotated slowly (1 revolution/second) while maintaining an aluminum source-sample distance of 8 cm. The source was at a 45° angle above the sample, which was oriented horizontally. Another set of samples was left uncoated and was examined at high sample tilt using Low Voltage Scanning Electron Microscopy (LVSEM).

As described earlier, conventional SEM requires that electrically- insulating samples be coated with a thin metal layer to avoid electron beam induced charging. However, if an SEM is operated at low accelerating voltages, typically less than 3.0 KV, the effects of charging can be greatly reduced and nonconducting samples may be examined without the customary metal coating.[19] This technique is referred to as LVSEM.

The absence of the metal coating eliminated the need to compensate for the coating's finite thickness in determining the contact diameter (a significant concern when dealing with small contacts) and also eliminated concerns about how, if at all, the coating affects the particle-substrate interaction.

The samples were examined using a Philips 515 SEM. The samples prepared for the CAM technique were examined at 0° tilt, 30 KV accelerating voltage, and with a 20 nm spot. The uncoated samples prepared for high tilt examination were viewed at 88° tilt, 3 KV accelerating voltage, and with a 10 nm spot size.

For additional verification, samples were also submitted to an outside lab[20] for independent high tilt measurements and analysis.

DISCUSSION AND RESULTS

Figure 1 shows SEM micrographs of the uncoated samples examined using the high tilt technique. Figure 1A shows a nominal 40 μm glass bead contacting a silicon substrate, and Figure 1B shows a higher magnification view of the contact zone. Figure 1C shows a nominal 8 μm glass bead contacting a silicon substrate, and Figure 1D shows a higher magnification view of the contact zone. Figure 2 shows SEM micrographs of the samples examined using the CAM technique. Figure 2A shows a nominal 8 μm glass bead on a silicon substrate and Figure 2B shows the contact zone after particle removal. Figure 2C shows a nominal 40 μm glass bead on a silicon substrate and Figure 2D shows the contact zone after particle removal. No permanent deformation of the silicon substrate was observed. The "bulls-eye" appearance of the contact zone is a characteristic of the CAM technique and results from the coating process. The outer area received the most coating material and appears bright. The outer annular ring is

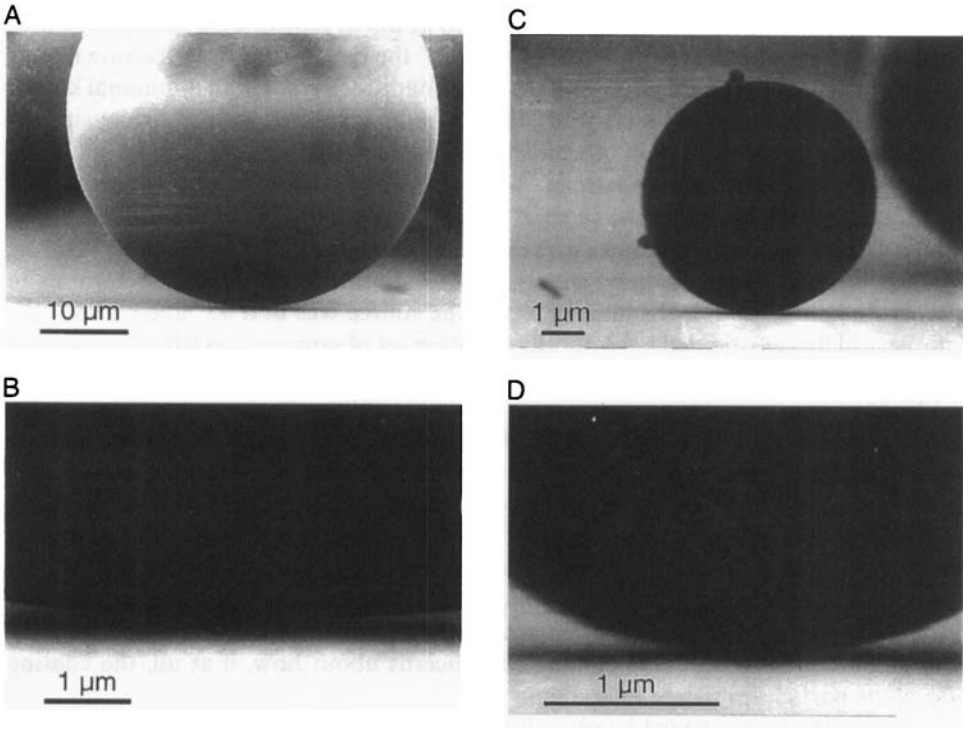

FIGURE 1 SEM micrographs of glass beads on silicon examined at an 88° sample tilt. Figure 1A shows a nominal 40 μm glass bead and Figure 1B shows the contact zone examined at higher magnification. Figure 1C shows a nominal 8 μm glass bead and Figure 1D shows the contact zone examined at higher magnification.

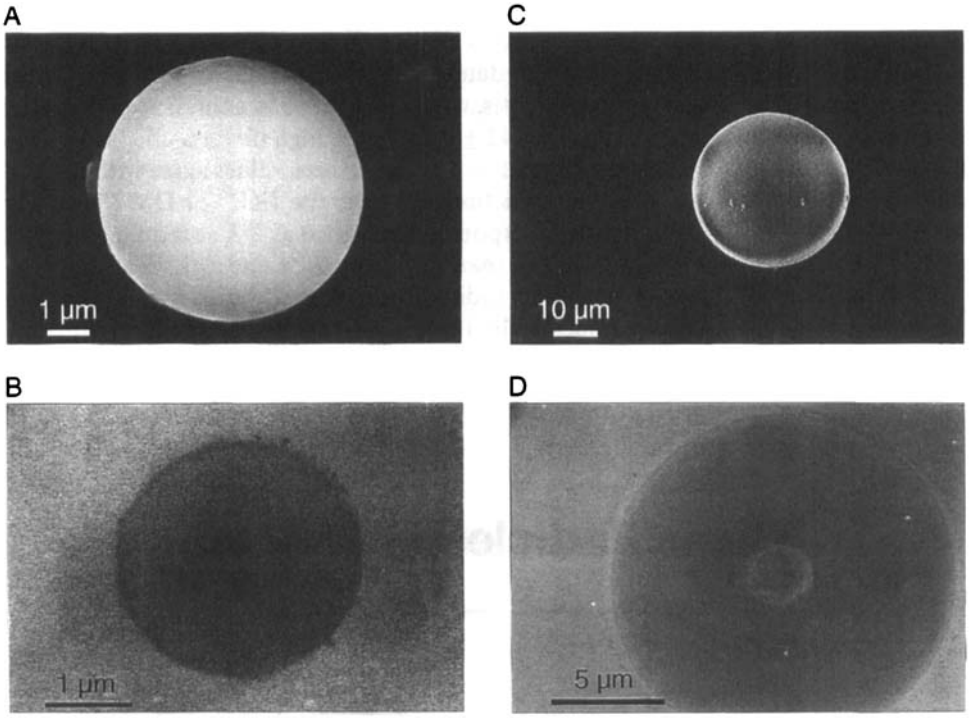

FIGURE 2 SEM micrographs of glass beads on silicon examined before and after bead removal using the CAM technique. Figures 2A and 2B show a nominal 8 μm bead before and after removal, respectively. Figures 2C and 2D show a nominal 40 μm bead before and after removal, respectively. The "bulls-eye" appearance of the contact zone seen in Figures 2B and 2D is a characteristic of the CAM technique and results from the coating process. The inner circle is the contact area.

dark because this area was shadowed from the direct influx of coating material by the particle. The inner circle is the contact area.[15] Table I summarizes the results for both the high tilt and CAM techniques. The number of beads examined, the average particle and contact radii and their respective standard deviations are listed for each size category of glass bead.

TABLE I
Summary of particle radius and contact radius data collected for glass beads on silicon wafer using the high tilt and CAM techniques. The measurements are quoted with a 95% confidence internal

Number of particles examined	Average particle radius (μm)	Average contact radius (μm)	Technique
6	2.74 (± 0.29)	0.25 (± 0.06)	high tilt
5	4.25 (± 0.79)	0.29 (± 0.09)	high tilt
6	21.01 (± 0.96)	0.58 (± 0.06)	high tilt
7	3.39 (± 0.44)	0.24 (± 0.10)	CAM
11	11.66 (± 0.95)	0.50 (± 0.03)	CAM
8	22.62 (± 0.88)	0.56 (± 0.12)	CAM

To determine the power law dependence of the contact radius on the particle radius, the data were plotted on a log-log scale. Figures 3A and 3B are plots of log contact radius *versus* log particle radius for the high tilt data and the CAM data, respectively. Linear regression analyses indicate that the slopes, with a quoted 95% confidence interval as determined using a Students t-test, are 0.42 ± 0.12 for the high tilt data and 0.43 ± 0.16 for the CAM data. Within the 95% confidence interval, these values agree with the MP model[10] but do not agree with the predictions of either the JKR[5] or DMT[6] models. Moreover, the probability that the true exponent be as great as 2/3, as required by JKR and DMT theories, was found to be less than 1% using the same statistical analysis.

Figures 4A and 4B are plots of contact radius *versus* particle radius to the 1/2 power for the high tilt and CAM data, respectively. These figures show the data approximately fit a straight line, indicating that the 1/2 relationship is reasonable. Also, the Y-intercepts indicate that there are minimal, if any, externally applied forces contributing to the adhesion contact.

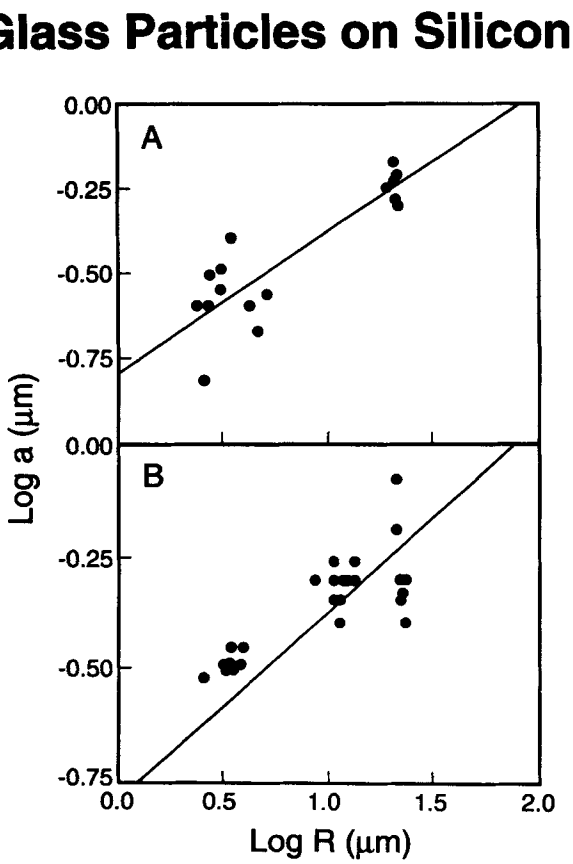

FIGURE 3 Plots of log contact radius, a, *versus* log particle radius, R, for the high tilt data (Fig. 3A) and the CAM data (Fig. 3B). The high tilt data has a slope of 0.42 ($\pm$ 0.12 with a 95% confidence interval). The CAM data has a slope of 0.43 ($\pm$ 0.15 with a 95% confidence interval).

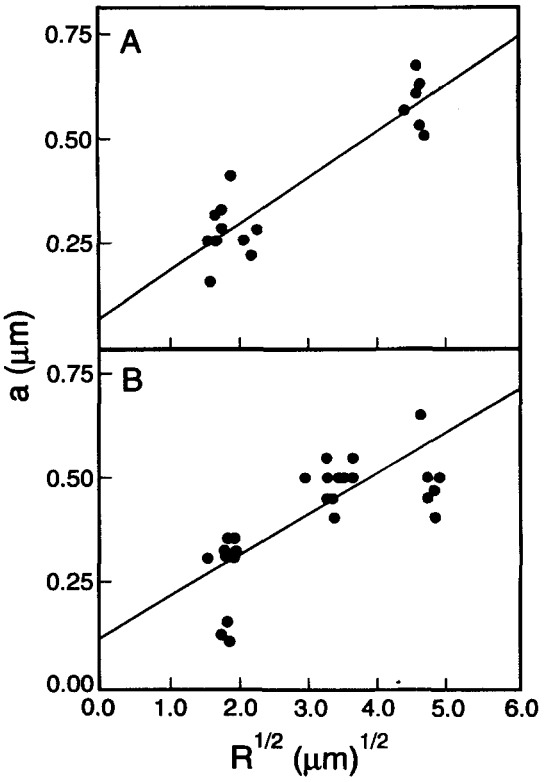

FIGURE 4 Plots of contact radius, a, *versus* particle radius, R, to the 1/2 power, for the high tilt data (Fig. 4A) and the CAM data (Fig. 4B). The least-squares approximately fits the data indicating that the 1/2 power relationship is reasonable.

Another approach to describe the nature of the deformation is to use the elastic and plastic response theories to calculate the work of adhesion, w_a. The first step is to determine that if the deformation were elastic in nature, would the JKR or DMT model better describe the deformation. Muller *et al.*[8] have shown that the appropriate regions of each theory can be distinguished by a dimensionless parameter, μ, where

$$\mu = \frac{32}{3\pi}\left[\frac{2R(w_a)^2}{\pi E^* z_0^3}\right]^{1/3} \tag{7}$$

and

$$\frac{1}{E^*} = \frac{(1-\nu_1^2)}{E_1} + \frac{(1-\nu_2^2)}{E_2}$$

E_i and ν_i are the Young's modulus and Poisson's ratio, respectively, of each material and z_0 is the separation distance between the particle and substrate (typically 0.4 nm for

van der Waals bonded crystals). If $\mu < 1$, the DMT model is more appropriate to describe the deformation, whereas, if $\mu > 1$, the JKR model should be used. Substituting reasonable values ($E_{glass} \approx E_{silicon} \approx 90$ GPA, $\nu_{glass} \approx \nu_{silicon} \approx 0.25$, $w_a = 0.1\,J/m^2$, $R = 10\,\mu m$) for the parameters in Equation (7) yields $\mu \approx 9000$. This suggests the system is describable by the JKR model. As discussed by Tabor,[7] the expression relating the contact radii and particle radii based on the JKR model is

$$a = \left(\frac{9\pi R^2 w_a (1 - \nu^2)}{2\ E}\right)^{1/3} \tag{8}$$

For a 10 μm radius particle and a 0.4 μm radius contact (the average particle radius for this study and its contact radius as determined from Figure 4) the work of adhesion calculated according to this model is 3.5 J/m^2. This is unrealistically large. If the DMT model were appropriate, the calculated work of adhesion would be an order of magnitude larger than that calculated from the JKR model. These results lend further strength to the argument that the deformations cannot be elastic. Assuming the occurrence of plastic flow, the work of adhesion can be calculated using the results of Maugis and Pollock.[10] The works of adhesion calculated from the slopes of the curves shown in Figures 4A and 4B are 0.69 J/m^2 and 0.55 J/m^2, respectively. These are in good agreement with each other and are reasonable values for this system.

Although direct observation of the deformations to the glass beads by dislodging and examining the contact zone would be desirable, manipulating micrometer size particles in a controlled manner is technically very difficult.

It is worthwhile to estimate the stresses on the particle due to the surface forces and to determine if they are sufficiently large to cause deformations. This can be done by assuming van der Waals type interactions. The force of the undeformed particle is

$$F_0 = 2\pi R w_a \tag{9}$$

For a 10 μm radius glass particle and an average $w_a = 0.62\,J/m^2$, $F_0 = 4 \times 10^{-5}$ N. However, as the size of the deformation increases, the surface forces increase until an equilibrium condition exists. The increase in the force can be estimated using an analysis proposed by Bowling.[21] The force on the deformed particle, F_d, is related to F_0 by

$$F_d = \frac{F_0 a^2}{z_0 R} \tag{10}$$

Substitution of the aforementioned values into Equation (10) yields an adhesion force of 2×10^{-3} N. The pressure exerted by the particle on the substrate is

$$P = \frac{F_d}{\pi a^2} = \frac{2w_a}{z_0} = 3 \times 10^9\ N/m^2 \tag{11}$$

The compressive strength of plate glass in 2.5×10^8 N/m^2 and the tensile strength is 4.5×10^7 N/m^2.[22] Another reference (23) indicates the tensile strength is 3.0×10^7 N/m^2 and that the tensile strength of glass is almost independent of composition. Although the corresponding strength for the soda lime glass particle used in this study is not known, it is probably comparable to plate glass. The compressive strength

of silicon is comparable to fused quartz. As can be seen, the pressure exerted by the 10 μm glass bead resting on silicon exceeds both the compressive strength and tensile strength of the glass.

CONCLUSIONS

The surface-force induced contact radii of glass beads, ranging from 3 to 25 μm in radius, on a silicon substrate, were determined using scanning electron microscopy. It was found that the contact radius varies with the particle radius to the 0.42 power (± 0.14 at the 95% confidence interval). This result is not consistent with the predictions of elastic response theories proposed by Johnson, Kendall, Roberts,[5] and Derjaguin, Muller, Toporov,[6] but is consistent with the predictions of the plastic response theory of Maugis and Pollock.[10] Further evidence suggesting the occurrence of plastic deformations is given by the works of adhesion calculated from these theories. Assuming plastic response, the average work of adhesion was calculated to be 0.62 J/m^2, which is reasonable. Alternatively, the works of adhesion calculated using the JKR and DMT models are 3.5 J/m^2 and 20.4 J/m^2, respectively. These values are unrealistically large. It is proposed that the observed plastic response results from the surface forces being sufficiently large to exceed the tensile and compressive strength of glass, and this induces plastic flow of the glass bead.

Acknowledgement

The authors would like to thank J. Morris for his statistical analysis of the data.

References

1. R. S. Bradley, *Philos. Mag.* **13,** 853 (1932).
2. R. S. Bradley, *Trans. Faraday Soc.* **32,** 1088 (1936).
3. B. V. Derjaguin, *Kolloid Z.*, **69,** 155 (1934).
4. H. Hertz, *Miscellaneous Papers* (Macmillan, London, 1986).
5. K. L. Johnson, K. Kendall and A. D. Roberts, *Proc. R. Soc. London A,* **324,** 301 (1971).
6. B. V. Derjaguin, V. M. Muller and Yu. P. Toporov, *J. Colloid Interface Sci.*, **53,** 314 (1975).
7. D. Tabor, *J. Colloid Interface Sci.*, **58,** 2 (1977).
8. V. M. Muller, V. S. Yushchenko and B. V. Derjaguin, *J. Colloid Interface Sci.*, **77,** 91 (1980).
9. H. Krupp, *Adv. Colloid Interface Sci.*, **1,** 111 (1967).
10. D. Maugis and H. M. Pollock, *Acta Metall.*, **32,** 1323 (1984).
11. D. S. Rimai, L. P. DeMejo and R. C. Bowen, *J. Appl. Phys.*, **68** (12), 115 (1990).
12. L. P. DeMejo, D. S. Rimai and R. C. Bowen, *J. Adhesion Sci. Technol.*, **11,** 959 (1991).
13. L. P. DeMejo, D. S. Rimai, J. Chen and R. C. Bowen, *J. Adhesion*, **39,** 61 (1992).
14. D. S. Rimai, L. P. DeMejo, W. B. Vreeland, R. C. Bowen, S. R. Gaboury and M. W. Urban, *J. Appl. Phys.*, **73,** 2 (1993).
15. R. C. Bowen, L. P. DeMejo, D. S. Rimai, *J. Adhesion*, this issue.
16. Duke Scientific Corporation, Palo Alto, California 94303.
17. L. N. Rogers and J. Reed, *J. Phys. D*, **17,** 677 (1984).
18. S. Wall, W. John and S. L. Goren in *Particles on Surfaces 2: Detection, Adhesion and Removal.* K. L. Mittal, Ed. (Plenum, New York, 1989).
19. J. Goldstein, D. Newbury, P. Echlin, D. Joy, A. Romig, C. Lyman, C. Fiori and E. Lifshin, *Scanning Electron Microscopy and X-Ray Microanalysis, 2nd Edition* (Plenum, New York, 1992).
20. H. Helbig and L. Kotoman, Clarkson University, private communications.

21. R. A. Bowling in *Particles on Surfaces 1*, K. L. Mittal, Ed. (Plenum, New York, 1988).
22. D. Miner and J. Seastone, "Handbook of Engineering Materials", in *Wiley Engineering Handbook Series* (Wiley and Sons, Inc., New York, 1955), pp. 4–152.
23. S. Schneider in *Engineered Materials Handbook*, Vol. 4, "Ceramics and Glasses" (ASM International, Metals Park, OH, 1991).